Operation of the Prospective ILC Beamline Calorimeter in the High-Radiation Forward Environment of the International Linear Collider

Bruce A. Schumm*, Benjamin Smithers

Santa Cruz Institute for Particle Physics and the University Of California, Santa Cruz, Santa Cruz California 95064

Work performed within the FCAL Collaboration

Abstract

Results on electromagnetically-induced radiation damage to silicon diode sensors, obtained from the T506 experiment at SLAC, are used in concert with detailed shower simulations to project the effects of radiation damage on the proposed International Linear Collider Beamline Calorimeter (BeamCal) detector system. The study makes use of the FLUKA Monte Carlo to simulate electromagnetic showers in both the T506 apparatus and the prospective BeamCal detector system. Under the conservative assumption that sensor leakage currents are dominated by the neutron component of the electromagnetic shower, and assuming that resulting leakage currents depend linearly on neutron fluence, the power consumption required to operate the BeamCal detector at a temperature of -10° C would be expected to increase by less than 100 W per year of operation. Lowering the operating temperature to -30° C would be expected to reduce the growth in power consumption to approximately 15 W per year. Results on fluences of both electromagnetic and hadronic particles in regions peripheral to the bulk of the BeamCal detector system, where front-end electronics would be mounted, are also presented.

Keywords: radiation damage, silicon diode sensor, forward calorimetry

*Corresponding author.
Email address: baschumm@ucsc.edu (Bruce A. Schumm)

1. Introduction

The International Linear Collider (ILC) [1] is designed to collide beams of high energy electrons and positrons for the purpose of performing precision measurements of the properties of Standard Model particles and interactions, as well as to search for signatures of new physics that are otherwise difficult to detect. Among such signatures are those for which the new physics is only accessible through states that are nearly degenerate to long-lived neutral states that carry off most of the collision energy. Such signatures are produced in competition with high cross section two-photon events for which the incoming electron and positron are only lightly deflected in the collision, leading to a minimal energy deposition in the central detector that mimics the limited visible energy of the degenerate new physics signatures.

Such background events can, in principle, be identified and rejected if one or more of the deflected beam particles are identified in the most forward system of the ILC detector: the prospective Beamline Calorimeter (BeamCal), which provides coverage at angles as close as five milliradians from the beam trajectory. However, for nominal ILC collision parameters [1], this instrument would be subjected to a radiation dose of approximately 10 TeV of electromagnetically-induced radiation per beam crossing, arising from the tens of thousands of electron-positron pairs created with each beam crossing. At the most irradiated point within the BeamCal instrument, the accumulated radiation dose is expected to exceed 100 Mrad of ionizing radiation per year.

Envisioned as a sampling calorimeter with a tungsten absorber, the chosen sensor material must withstand the intense ionizing particle fields induced by the pair background showering in the tungsten. Potentially more damaging, though, is the flux of neutrons that arise primarily from the de-excitation of the giant dipole resonance of the tungsten nuclei that is stimulated by the absorption of photons in the shower that are close to tungsten's critical energy. The associated radiation dose can lead both to the development of leakage current, resulting in quiescent power draw, as well as a loss of signal-collection efficiency.

To assess the damaging effect of tungsten-induced electromagnetic showers on various candidate solid-state sensor materials, the Santa Cruz Institute for Particle Physics (SCIPP) conducted experiment T-506 in the SLAC End Stations A Test Beam (ESTB) facility. In this experiment, for which results have been reported elsewhere [2], a multi-GeV electron beam was di-

rected onto a tungsten radiator, in the midst of which (at shower max) a series of candidate sensors were inserted and exposed to doses of up to 600 Mrad of electromagnetically induced radiation. While the use of a tungsten radiator to surround the candidate sensor produced a realistic shower, containing both electromagnetic and hadronic components, both the energy and angular profile of the T-506 radiation field, as well as the overall exposure rate, are different from that of the radiation field expected to illuminate the BeamCal instrument. The purpose of this study was to use the FLUKA simulation package [3, 4, 5], combined with conventional assumptions about the radiation field energy profile dependence and the exposure dependence of the observed T-506 damage, to estimate the effects of the pair-background-induced radiation field on the performance of a BeamCal constructed with silicon diode sensors. The simulation results will be presented in general enough form that radiation damage studies of other materials, whether from T-506 or other experiments, can also be used to estimate the performance of those materials under prolonged use in the BeamCal instrument.

2. The ILC and the Beamline Calorimeter

The International Linear Collider (ILC), if constructed, is expected to collide trains of beams of high-energy electrons and positrons at a rate of 5 Hz. The design energy, bunch separation within the train, number of bunches within a train, and bunch charge are subject to change as the design of the ILC matures and evolves to meet sharpening physics goals as well as practical and political constraints. For this study, we assume the baseline parameters presented in the Technical Design Report [1], for which a train consists of 1312 colliding bunches, each separated by 554 nsec from the preceeding bunch collision, and with a luminosity of 3.6 nb^{-1} per bunch collision. The flux of electron and positron pairs arising from the bunch collisions is simulated with the GUINEA-PIG [6] Monte Carlo program, initialized to reflect the collision parameters of the TDR baseline beam.

The current baseline design for the ILC Beamline Calorimeter (BeamCal) consists of a tungsten sampling calorimeter read out by planes of solid-state pad detectors. The calorimeter is composed of 50 tungsten plates of thickness 2.5 mm, with a radius (in the plane transverse to the beam direction) of 15 cm. In the version simulated here, each plate is punctuated by two circular holes, one each to accommodate the incoming and outoing beampipes, which diverge from each other with an angle of 14 mrad in the plane formed by the

horizontal (x) and beam (z) axes. The hole accommodating the incoming beampipe has a radius of 1.55 cm, while the hole accommodating the outgoing beampipe has a radius of 2.05 cm, somewhat larger than that of the incoming beampipe to allow for the effects of disruption when the beams collide. At the face of the BeamCal (surface facing the ILC interaction point), the centers of the two holes are separated by 4.57 cm. The BeamCal is centered on the outgoing beamline at a distance of 326.5 cm from the interaction point, providing an angular coverage between 5 and 45 mrad. Figure 1 depicts the basic geometrical features of the BeamCal.

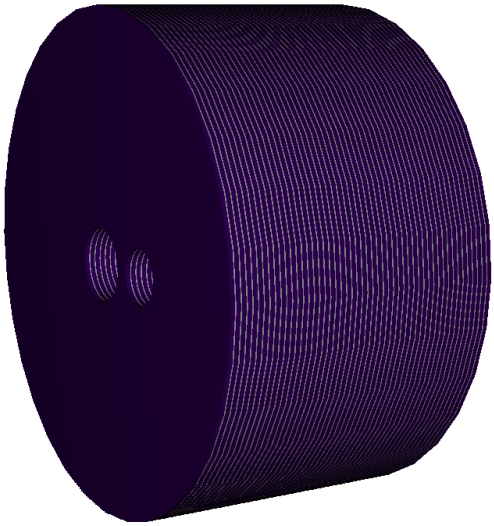

Figure 1: Geometry of the BeamCal instrument within the FLUKA simulation. This plot was produced using the visualizatoin package within SimpleGeo [7].

3. The T-506 Experiment

The T-506 Experiment, whose results on the radiation damage to solid-state sensors provide the empircal input to FLUKA-based estimates of BeamCal degradation during operation at the ILC, was mounted in the SLAC accelerator laboratory's End Station A Test Beam (ESTB) facility. The T-506 target consisted of a 2 X_0 upstream radiator (R1) that initiatied the shower, followed by a 4 X_0 radiator (R2) that brought the electromagnetic shower to maximum intensity. The candidate sensor was mounted immediately behind

R2, followed immediately in turn by an 8 X_0 radiator (R3). The locations and thicknesses of the T-506 target elements are provided in Table 1. Mounting the sensor in the immediate proximity of tungsten radiators insured that a significant hadronic component accompanied the electromagnetic particles in the shower. More details about the exposure of candidate sensors, and their characterization both before and after irradiation, can be found in [2].

Table 1: Location of the various tungsten radiator elements and the sensor under irradiation for the phase of T-506 running in which the WSI-P4 sensor was irradiated. The R1 radiator had a thickness of 2 X_0, the R2 radiator 4 X_0 and the R3 radiator 8 X_0.

Surface	Location (cm)
R1 Entrance	0.0
R1 Exit	0.7
R2 Entrance	46.6
R2 Exit	48.0
Sensor	48.5
R3 Entrance	49.4

Of particular interest to this work was the 2015 exposure of sensor WSI-P4, a $1.6\times1.6\times0.32$ mm^3 p-type float-zone bulk test structure associated with a prototype sensor developed for the ATLAS upgrade tracker [8]. In this exposure, 51 μC of 13.3 GeV electrons were directed onto the T-506 target over a period of approximately one day, corresponding to an accumulated dose of ionizing radiation of approximately 270 Mrad. The sensor was irradiated at close to 0° C and kept well below freezing subsequent to irradiation. The sensor's leakage current and charge collection efficiency were then evaluated after a series of one-hour annealing steps at successively higher temperature. The charge-collection measurement made use of a readout with an electronic shaping time of approximately 300 ns. While the post-irradiation leakage current was not changed significantly by the annealing episodes, for temperatures up to 80° C annealing was observed to lower the irradiated sensor's depletion voltage. At a bias of 600 V, close to full depletion after the 60° C annealing step, the charge collection efficiency was observed to be 80% of its un-irradiated value. The area density $\sigma(T)$ of the leakage current for the irradiated WSI-P4 sensor, at a bias of 600 V, is displayed as a function of temperature in Figure 2. The fit to the data shown in this figure has the

temperature dependence

$$\sigma(T) = ae^{T/T_s},$$

with the temperature scale constant T_s given by $T_s = 9.2°$ C and with the current density scale constant a given by 220 $\mu A/cm^2$. This dependence will be made use of in the esimatates of the power draw of the irradiated BeamCal presented below.

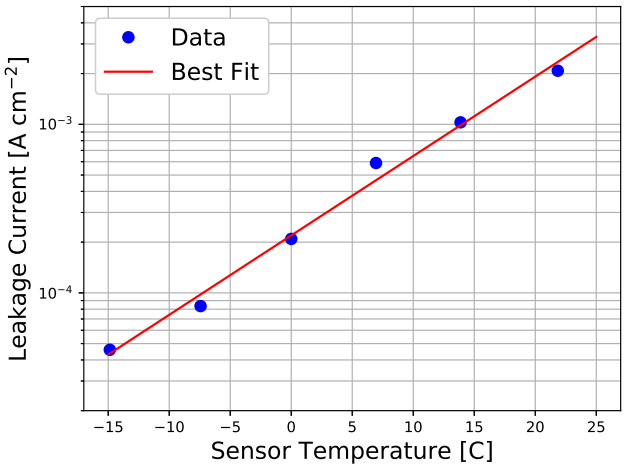

Figure 2: Observed temperature dependence of the area current density of the WSI-P4 silicon diode sensor, after irradiation.

4. FLUKA Simulation and the Exposure Metric

Both the T-506 target and BeamCal design were implemented in FLUKA. To enable neutron production through the evaporation of excited nuclear resonances, the "SDUM" argument for the FLUKA "PHYSICS" control card was set to the value "EVAPORAT"; the new FLUKA model of evaporation without heavy fragmentation was implemented through the use of the value "2" for the "WHAT(1)" argument of the "PHYSICS" card. To provide the maximum precision in the modeling of neutrons arising within the electromagnetic shower, the "SDUM" argument was set to the value "PRECISIO" for the "DEFAULTS" card. To improve the computing efficiency of the FLUKA simulation, a bias factor of +0.09 was applied to interaction frequency of electrons, positrons and photons with the tungsten nuclei via the

use of the "WHAT(2)" through "WHAT(5)" arguments of the "LAM-BIAS" card. Photonuclear interactions themselves were enabled by activating all available options of the "PHOTONUC" card. With FLUKA configured in this manner, low-energy neutron transport was modeled down to thermal energies.

The model of the T-506 target that was implemented in the FLUKA simulation is described in Table 1. FLUKA was then used to simulate 3×10^5 electromagnetic showers induced by incident electrons of energy 13.3 GeV. To simulate the rastering of the target during the T-506 exposure, the incident flux was distributed evenly within a square of side one cm, oriented transverse to the incident beam direction.

The BeamCal device was modeled as a set of 50 alternating layers of pure tungsten plates of thickness 2.5 mm and pure silicon sensors of thickness 300 μm, with each tungsten plate separate by 700 μm. Showers from electrons and positrons expected to arise from a single ILC beam crossing, assuming the nominal beam parameters [1], were simulated; the flux of electrons and positrons arising from the beam crossing was generated using the GUINEA-PIG MC program. This electron/positron flux consisted of approximately 5×10^4 incident charged particles, with a mean energy of 2.5 GeV and a high-energy tail extending to beyond 100 GeV. This simulated flux of particles incident on the BeamCal was highly peaked in the plane transverse to the beam direction, with the maximum of the distribution falling close to the inner edge of the exhaust beam cutout. The simulated electromagentic flux in the 8^{th} sensor layer, close to the peak of the resulting distrubution of electromagnetic shower particles, is shown in Figure 3.

The FLUKA simulation provides an accounting of the fluence Φ of particles traversing a given "scoring plane" of finite area A and infinitessimal width dz, with the fluence Φ defined as

$$\Phi = \frac{l}{Adz},$$

where l is the sum of all path lengths traversing the scoring plane's infinitessimal volume Adz. A single particle with angle of incidence θ passing through a scoring plane of area A thus has a fluence of $\Phi = 1/(A \cos\theta)$, with a physical unit of cm^{-2}. FLUKA can be configured to provide the differential fluence distribution in a two-dimensional grid of energy (E) and angle of incidence (θ) of shower particles relative to the normal of the scoring plane.

According to the non-ionizing-energy-loss (NIEL) scaling hypothesis [9],

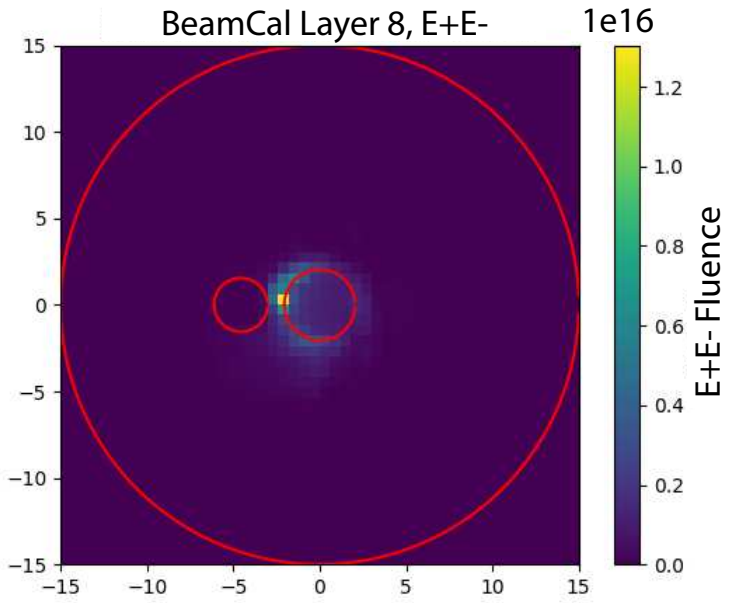

Figure 3: Estimated electromagnetic (electron and positon) fluence, in cm^{-2}, at the maximum of the electromagnetic shower in the BeamCal instrument, per 10^7 seconds of ILC operation. The esimated maximum occurs in the eigth sensor layer.

radiation damage in solid-state sensors is proportional to the deposition of energy in the sensor through processes other than ionization, i.e., processes in which the nuclei, rather than the electronic states, absorb energy from the incident radiation. In this study, we are particularly interesting in NIEL due to the flux of neutrons that arise within the electromegnetic shower itself. Because these neutrons are largely due to the excitation of the giant diople resonance, whose subsequent decay produces an isotropic distribution of neutrons relative to the decaying nucleus, the neutron-induced NIEL dose is much more pervasive within the BeamCal device than is the more ballistic electromagnetically-induced NIEL dose. The assumption that the radiation damage observed in T-506 is dominated by neutron-induced NIEL is thus conservative with respect to the projected performance of the BeamCal instrument after exposure to radiation.

The neutron-induced NIEL dose $N_n(E)$ per unit path length depends on the energy of the through-going neutron. The function $N_n(E)$ is well known

for neutrons passing through silicon, and is tabulated in [9] in terms of MeV of neutron-induced NIEL per g/cm^2 of silicon traversed per through-going neutron (see Figure 4). The quantity $\rho N_n(E)$, where $\rho = 2.33$ g/cm^3 is the mass density of silicon, thus provides the neutron-induced NIEL in terms of MeV per cm of traversed silicon. For a given bin of extent $\Delta E \Delta\Omega$ centered around an energy E and incident angle θ of neutrons traversing the scoring volume, the contribution ΔE_{NIEL} to the neutron-induced NIEL in the scoring plane volume is thus given by

$$\Delta E_{\mathrm{NIEL}} = \rho N_n(E) \frac{d^2 l}{dE d\Omega}(E, \theta) \Delta E \Delta\Omega$$

in units of MeV of neutron-induced NIEL; again, l is the total path length of neutrons through the scoring plane volume. More applicable, however, is the neutron-induced NIEL per unit of scoring plane volume due to neutrons in the given energy and angle bin, given by

$$\Delta\lambda = \frac{\Delta E_{\mathrm{NIEL}}}{A dz} = \rho N_n(E) \frac{d^2\Phi}{dE d\Omega}(E, \theta) \Delta E \Delta\Omega$$

in units of MeV of neutron-induced NIEL per cm^3 of scoring-plane volume, which makes explicit use of the double-differential fluence distribution $d^2\Phi/dEd\Omega$ provided by FLUKA. Note that in this discussion of NIEL, the energy E is that of the given shower particle (neutron) that is incident on the scoring plane buried within the apparatus, and not the energy of the particle (electron or positron) that initiates the shower.

The total exposure λ, again in terms of MeV of neutron-induced NIEL per cm^3 of scoring-plane volume, is then given by summing over all bins in angle and energy:

$$\lambda = \sum_{i=1}^{N_{bins}} \rho N_n(E_i) \frac{d^2\Phi}{dE d\Omega}(E_i, \theta_i) \Delta E_i \Delta\Omega_i.$$

For this study, simulated neutrons incident upon the scoring plane were binned in 60 uniform bins of $\Delta\Omega$, each of width $\pi/15$, and 336 logarithmically-varying bins of energy between 1×10^{-5} eV and 100 GeV.

5. Estimated Dose for T506 and Expected Leakage Current

The FLUKA simulation of the T506 geometry, as described above, was used to estimate the neutron-induced NIEL dose accumulated by the WSI-P4

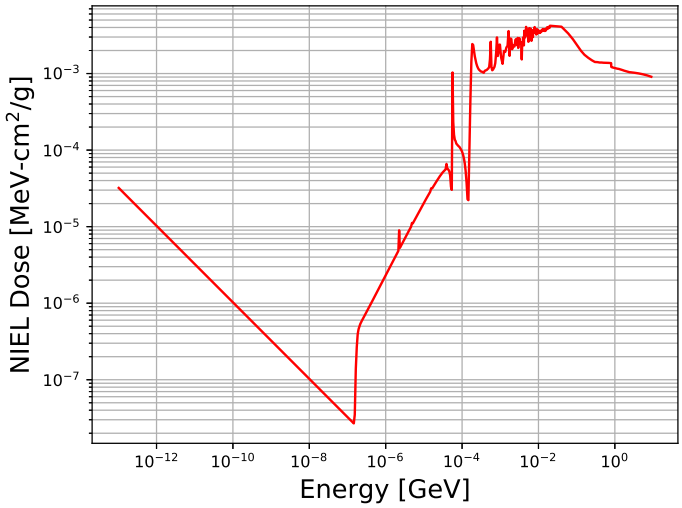

Figure 4: Energy dependence of neutron-induced NIEL in silicon, in MeV per g/cm^2 of silicon traversed per through-going neutron. This plot displays the data tabulated in [9].

sensor during its exposure in the T506 experiment. A total of 3×10^5 13.3 GeV electron showers were simulated with FLUKA. Figure 5 shows the energy distribution dN/dE of the simulated neutron flux, per incident 13.3 GeV electron, that traverses the sensor. Figure 6 shows the differential neutron-induced NIEL dose distribution $d\Phi/d\Omega$ as a function of neutron angle of incidence for the FLUKA simulation of the full WSI-P4 exposure. Due to the ballistic nature of the electromagnetic shower, the neutron fluence arises primarily from the region of the 1 cm^2 beam profile in the radiator immediately before and after the WSI-P4 sensor. As a result, the dose distribution is dominated by neutrons entering either the front or the back of the sensor with lower angles of incidence. Summing over all incident angles, and scaling to the delivered charge of 51 μC of 13.3 GeV electrons, yields an estimate of the total neutron-induced NIEL dose of 2.7×10^{11} MeV/cm^3 in the WSI-P4 sensor. For comparisons with the projected BeamCal dose, this amount of neutron NIEL is defined to be the "T506 dose unit" λ_{T506}.

As a point of comparison, studies of silicon diode detector leakage current arising from neutron irradiation have been performed by the CERN RD48 Collaboration [10]. RD48 explored a broad range of silicon diode detector technologies exposed to varying levels of neutron radiation, and found a

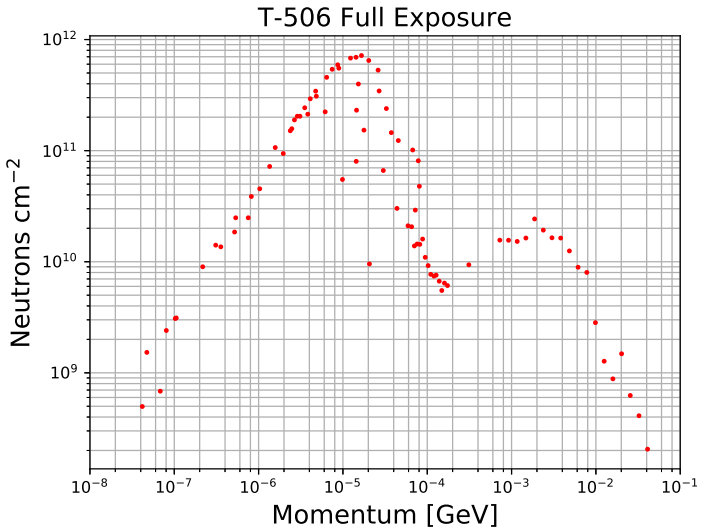

Figure 5: FLUKA estimate of the neutron fluence per 13.3 GeV primary, as a function of incident neutron energy, through the sensor scoring plane for the T506 experiment.

consistent linear dependence of the leakage current draw upon irradation dose. In terms of the 1-MeV equivalent neutron fluence Φ_{eq}, defined as

$$\Phi_{eq} = \int \frac{d\Phi}{dE}(E)\frac{N_n(E)}{N_n(1\text{MeV})}dE,$$

RD48 found that operating at a temperature of -10° C after an 80 minute annealing step at 60° C, the current draw in amps could be approximated as

$$I = \alpha\Phi_{eq}V,$$

where V is the volume of the sensor bulk in cm^3, and with the current proportionality constant α given by

$$\alpha_{RD48} = 4.0 \times 10^{-17} \text{ A/cm}.$$

The FLUKA simulation of the T506 target, combined with the energy-dependent neutron-induced NIEL values from [9], yielded an estimate of $\Phi_{eq} = 0.19$ cm^{-2} per 13.3 GeV primary, leading to an estimate of

$$\Phi_{eq}^{\text{T506}} = 6.0 \times 10^{13} \text{ cm}^{-2}$$

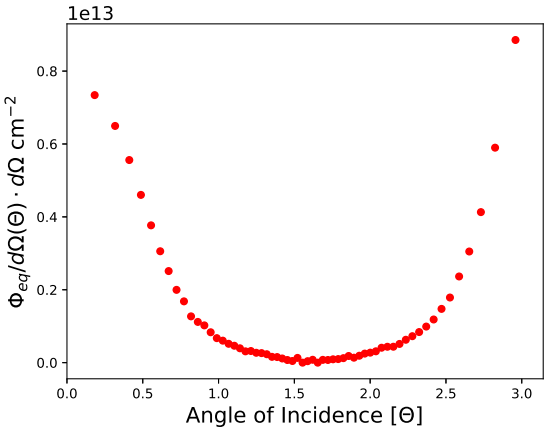

Figure 6: FLUKA estimate of the angular dependence of the 1 MeV-equivalent neutron fluence through the sensor scoring plane for the full exposure of the T506 experiment.

for the 51 μC T506 exposure. Based on the results of the RD48 leakage damage study, this leads to an expectation of 72 μA per cm^2 of detector area for the 300 μm-thick WSI-P4 sensor, operating at a temperature of -10° C. From Figure 2, the current observed in the WSI-P4 sensor at -10° C was 74 μA/ cm^2, close to the expected value of 72 μ/cm^2. Equivalently, the current draw in the WSI-P4 sensor can be characterized by a current proportionality constant of

$$\alpha_{T506} = 4.2 \times 10^{-17} \text{ A/cm}.$$

The near-agreement between the values of α_{RD48} and α_{T506} supports the hypothsis that the radiation damage suffered by the WSI-P4 sensor is dominated by neutron-induced NIEL.

6. BeamCal NIEL Dsitribution

The FLUKA package was used, as described above, to simulate the neutron field over the breadth and depth of the prospective ILC Beamline Calorimeter. The resulting energy distribution of neutrons in Layer 12 of the BeamCal, for a scoring plane centered on the maximum of the electromegnetic component of the expected shower profile (see Figure 3), is shown in Figure 7. Layer 12 is close to the peak depth of the neutron fluence distribution for the ILC-induced showers. The distribution is very similar to that observed for the T506 scoring plane (Figure 5).

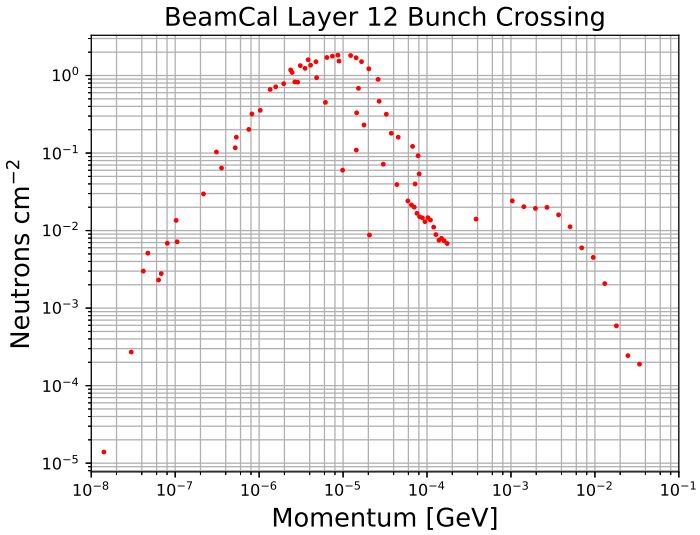

Figure 7: FLUKA estimate neutron flux, as a function of incident neutron energy, through the sensor scoring plane for Layer 12 of the BeamCal instrumtent, per ILC beam crossing. The distribution shows is that for a scoring plane centered on the maximum of the electromegnetic component (see Figure 3).

Figure 8 and Figure 9 (left) show the differential neutron-induced NIEL dose distribution $d\Phi/d\Omega$ as a function of neutron angle of incidence, per 10^7 seconds of ILC operation, for three locations in Layer 12 of the BeamCal. The three displayed locations are widely separated, including a point in the center of Layer 12, as well as one 24.1 mm beyond the outer edge of the exhaust (larger) circular cutout and one 34.2 mm beyond the outer edge of the incoming (smaller) circular cutout. Figure 9 (right) shows $d\Phi/d\Omega$ averaged over the entire layer. Reflective of the more distributed flux of electromagnetic particles on the face of the BeamCal, and the isotropic nature of the dominant source of neutrons in the shower (evaporative de-excitation of the giant dipole resonance in tungsten), the neutron fluence distribution is much more evenly spread out over solid angle than that of the T506 fluence distribution (Figure 6). As a result, the neutron fluence decreases much less rapidly with transverse distance from the axis of the shower peak than does the electromagnetic fluence. This leads, in turn, to the possibility that the overall power draw of a BeamCal instrumented with silicon diode detectors may lead to a prohibitive dissipative heat load after operation in the ILC

beam. Results on the projected BeamCal power draw are presented in the next section.

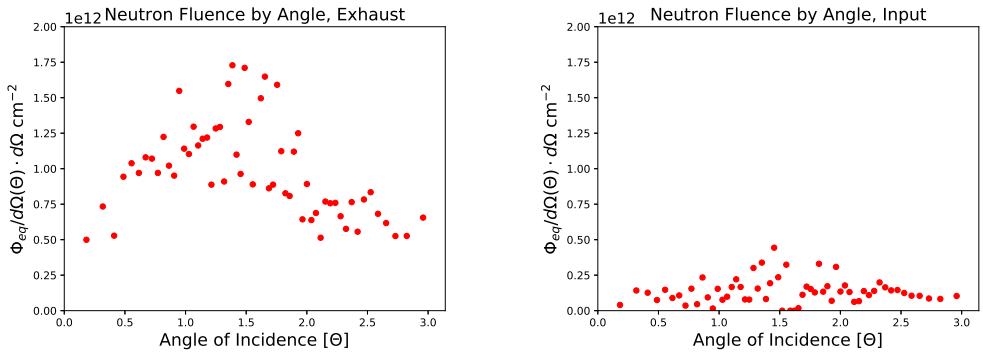

Figure 8: FLUKA estimates of the angular dependence of the 1 MeV-equivalent neutron fluence through scoring planes in Layer 12 of the BeamCal, for 10^7 seconds of ILC operation. Left: fluence distribution for a scoring plane 24.1 mm beyond the outer edge of the exhaust (larger) circular cutout. Right: fluence distribution for a scoring plane 34.2 mm beyond the outer edge of the incoming (smaller) circular cutout.

A series of scoring planes were configured across a section of the BeamCal at the depth of Layers 12 and 30, including those represented in Figures 8 and 9. For each scoring plane, the neutron-induced NIEL per ILC beam crossing was estimated. This result was then scaled up by the product of factors of 1312 (the number of ILC beam crossings per second) and 10^7 (the estimated number of second of operation per year) to provide an estimated neutron-induced NIEL per year of ILC operation. Figures 10 and 11 show the neutron-induced NIEL results for these various scoring planes in Layers 12 and 30, respectively. The results are expressed in terms of the T506 dose unit λ_{T506} described above. The neutron-induced NIEL profile is seen to fall off much less rapidly with distance from the center of the BeamCal than the corresponding electromagnetically-induced deposition (see Figure 3). Thus, an assumption that leakage-current inducing radiation damage is dominated by nutron-induced NIEL is conservative with respect to the total estimated leakage current (and resulting power draw) for the irradiated BeamCal instrument.

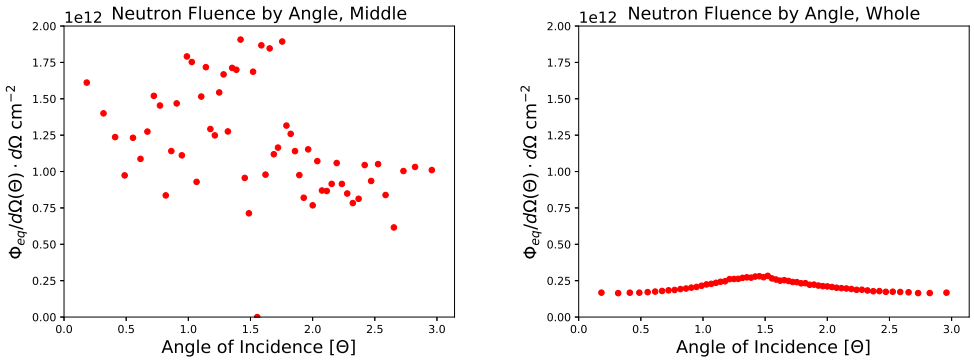

Figure 9: FLUKA estimate of the angular dependence of the 1 MeV-equivalent neutron fluence through scoring planes in Layer 12 of the BeamCal, for 10^7 seconds of ILC operation. The distribution shown in the left plot is that for a scoring plane at the center of the BeamCal, i.e., at the peak of the electromagnetic flux shown in Figure 3. The right plot shows the average of the distribution over the full layer.

7. Expected Power Draw After Irradiation

By introducing a single scoring plane comprising the entire surface of a given BeamCal layer's sensor plane, FLUKA can be configured to accumulate the mean differential fluence $d^2\Phi_L/dEd\Omega$ through the entire detector layer for a given duration of ILC operation with nominal beam parameters. This can then be turned into a mean neutron-induced NIEL energy-deposition density λ_L as outlined in Section 4. Assuming a linear dependence of leakage current upon neutron-induced NIEL dose, the total leakage current through the given layer, for a bias of $V_B = 600$ V and an operating temparature T, can then be estimated as

$$I_L(T) = \frac{\lambda_L}{\lambda_{T506}} A\sigma(T),$$

where A is the sensor surface area, $\sigma(T)$ is the area current density measured for the irradiated WSI-P4 sensor (see Figure 2), and $\lambda_{T506} = 2.7 \times 10^{11}$ MeV/cm^3 is the neutron-induced NIEL dose accumulated by the WSI-P4 sensor. Here, it is assumed that the thickness of the BeamCal sensor is the same as that of the WSI-P4 sensor (300 μm). The total power draw $P_L(T)$ in the layer is then given by multiplying the current draw $I_L(T)$ by the bias voltage:

$$P_L(T) = V_B I_L(T) = V_B \frac{\lambda_L}{\lambda_{T506}} A\sigma(T).$$

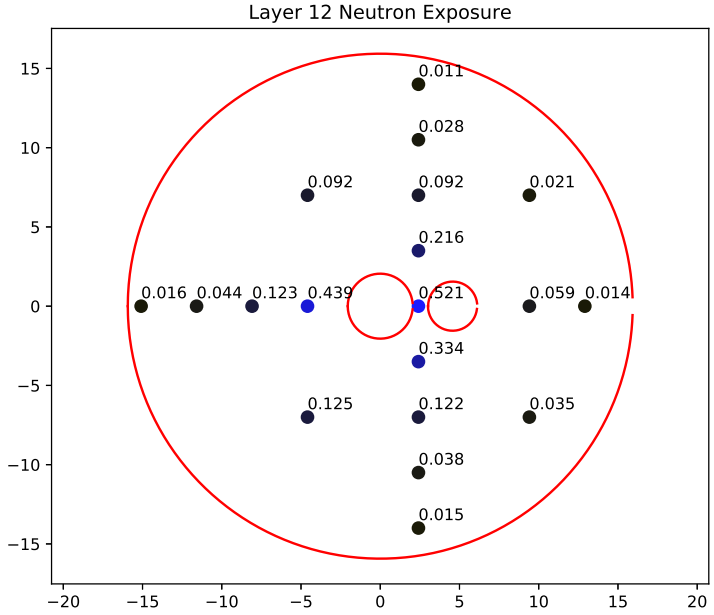

Figure 10: FLUKA estimate of neutron-induced NIEL for the various scoring planes configured for Layer 12 of the BeamCal. The results are shown per year of ILC running (as defined in the text), and expressed in terms of the T506 dose unit λ_{T506}.

Figure 12 show the resulting estimate for $P_L(T)$ as a function of layer for a series of operating temperatures between -15° C and 22° C, for 10^7 seconds of operation at the ILC.

The maximum power dissipation density will arise approximately at the peak of the electromagnetic (electron and positron) deposition distribution in Layer 12 of the BeamCal. At this point, after 10^7 seconds of exposure in the ILC and operating at a bias voltage of 600 V and a temperature of -10° C, the power draw is approximately 23 mW per cm^2 of sensor area.

Having estimated the layer-by-layer current draw as a function of operating temperature, the total power draw is then giving by summing the power draw over all layers. Figure 13 shows the total expected power draw as a function of temperature; the expected power draw after roughly 1 year of ILC operation varies between 40 and 2500 W for temperatures between -20° and 20° C, and would be of order 15 W for an operating temperature of -30° C.

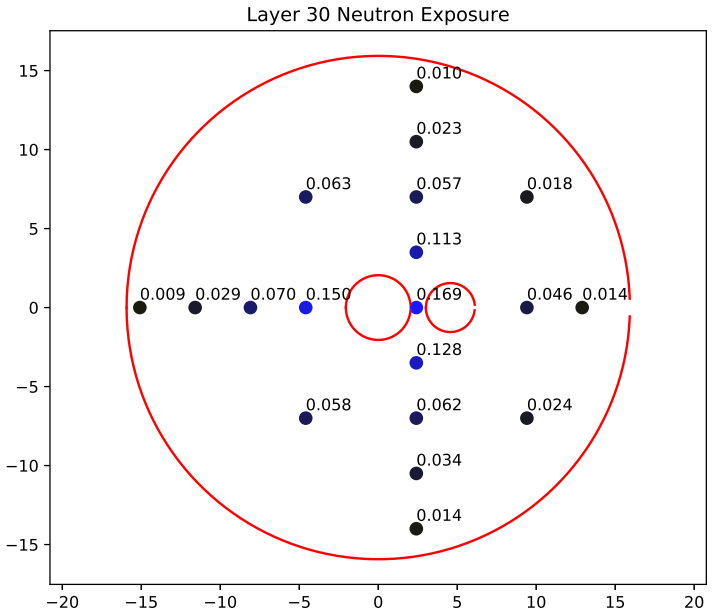

Figure 11: FLUKA estimate of neutron-induced NIEL for the various scoring planes configured for Layer 30 of the BeamCal. The results are shown per year of ILC running (as defined in the text), and expressed in the T506 dose unit.

8. Peripheral Flux Calculations

The BeamCal front-end electronics is likely to be mounted just outside the BeamCal structure. Thus, FLUKA has also been used to estimate neutron and electromagnetic particle fluences in regions immediately peripheral to the BeamCal instrument.

Table 2 shows the expected neutron fluence per nominal year of operation, for scoring planes oriented transverse to the beam direction, at various points 1 cm outside the BeamCal instrument. The corresponding electromagnetic fluence was found to be less than 10^{11} through-going charged particles (electrons and positrons) per cm^2 per nominal year at any of these positions.

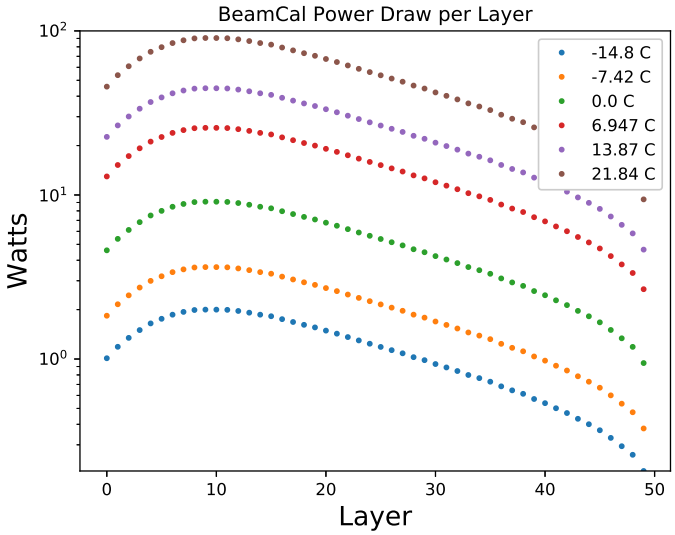

Figure 12: Expected power draw per layer for operation with a bias volatge of $V_B = 600$ V after 10^7 seconds of operation in the ILC, for various operating temperatures.

Table 2: Neutron fluences at various positions 1 cm outside the BeamCal instrument, for 10^7 seconds of ILC operation, in cm^{-2}. The angle is measured relative to the axis defined by the center of the BeamCal and the centerline of the smaller circular cutout.

Angular position	0	$\pi/2$	π	$3\pi/2$
Layer 12 fluence (cm^{-2})	4.9×10^{11}	5.9×10^{11}	7.3×10^{11}	8.0×10^{11}
Layer 30 fluence (cm^{-2})	4.8×10^{11}	4.6×10^{11}	5.7×10^{11}	5.4×10^{11}

9. Summary and Conclusions

Making use of the FLUKA simulation package, projections have been made of the performance of the Beamline Calorimeter instrument after exposure to beam-induced radiation from the prospective International Linear Collider. These projections were normalized to the observed performance of a prototype p-type, float-zone bulk prototype silicon diode detector exposed to electromagnatically-induced radiation in experiment T506 at the SLAC End Station Test Beam facility. The projections were based on the conservative assumption that damage to silicon diode sensors is dominated by the neutron component of the electromagnetic shower, which is supported by the

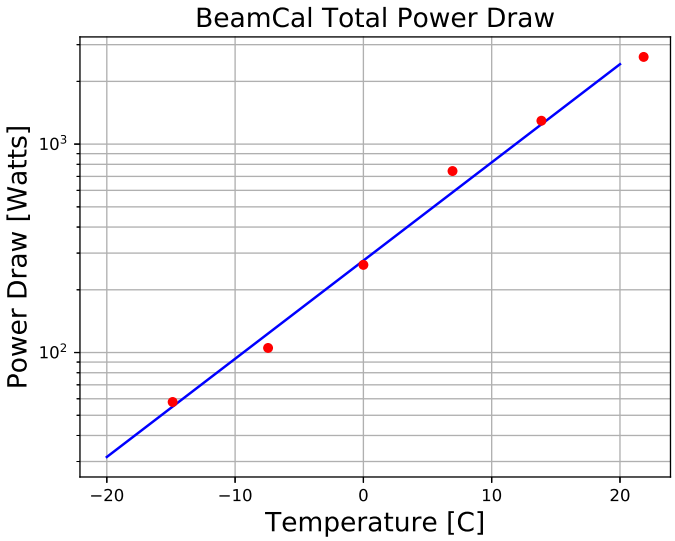

Figure 13: Expected power as a function of temperature for the entire BeamLine Calorimeter instrument, for operation with a bias volatge of V_B = 600 V and a temperature of T = -10° C, after 10^7 seconds of operation in the ILC.

comparison of the T506 leakage current results with expectations from prior radiation damage studies.

The T506 studies suggest that after several years of exposure of a Beamline Calorimeter instrumented with silicon diode sensors, for sufficient bias voltage the charge collection will remain high (50% or greater) even in the most heavily-irradiated portions of the Beamline Calorimeter. Assuming operation at a bias voltage of 600 V and a temperature of -10° C, the overall power draw of the Beamline Calorimeter will increase by less than 100 W per year of operation. Lowering the operating temperature to −30° C would be expected to reduce the growth in power consumption to approximately 15 W per year. Finally, both charged and neutral particle fluences in the region just outside the Beamline Calorimeter instrument, where the front-end electronics would be mounted, were estimated to be at levels that would be unlikely to pose a threat to the performance of the readout.

10. Role of the Funding Source

The work described in this article was supported by the United States Department of Energy, grant DE-SC0010107. The funding agency played no

role in the design, execution, interpretation, or documentation of the work described herein.

References

[1] Behnke, T. et al. [ILC Collaboration], *The International Linear Collider Technical Design Report*, 2013, arXiv:1306.6327 [physics.acc-ph].

[2] P. Anderson et al., *Updated Results of a Solid-State Sensor Irradiation Study for ILC Extreme Forward Calorimetry*, Proceedings of the LCWS2016 International Workshop on Linear Colliders, Morioka City, Iwate, Japan, December 5–9, 2016, arXiv:1703.05429.

[3] A. Ferrari, P. R. Sala, A. Fassò and J. Ranft, *FLUKA: A multi-particle transport code* (program version 2005), CERN Yellow Report https://cds.cern.ch/record/898301, 2005.

[4] T.T. Böhlen et al., *The FLUKA Code: Developments and Challenges for High Energy and Medical Applications*, CERN-2005-10 (2005), INFN/TC_05/11, SLAC-R-773.

[5] V. Vlachoudis, *FLAIR: A Powerful But User Friendly Graphical Interface For FLUKA*, Proc. Int. Conf. on Mathematics, Computational Methods & Reactor Physics (M&C 2009), Saratoga Springs, New York, 2009, http://www.fluka.org/flair/.

[6] D. Schulte, *Study of Electromagnetic and Hadronic Background in the Interaction Region of the TESLA Collider*, PhD thesis, DESY, 1997.

[7] C. Theis et al., *Interactive three dimensional visualization and creation of geometries for Monte Carlo calculations*, Nucl. Inst. & Meth. **A562**, 827, 2006, http://theis.web.cern.ch/theis/simplegeo/.

[8] Y. Unno et al, *Development of n-on-p silicon sensors for very high radiation environments*, NIM A 636, S24 (2011).

[9] A. Vasilescu and G. Lindstroem, *Displacement damage in silicon, on-line compilation*, 2006, http://rd50.web.cern.ch/RD50/NIEL/default.html.

[10] G Lindström et al., *Radiation hard silicon detectors - developments by the RD48 (ROSE) collaboration*, Nucl. Inst. & Meth. **A466**, 308, 2001, http://dx.doi.org/10.1016/S0168-9002(01)00560-5.